



ELSEVIER

Brain Research 663 (1994) 206–214

**BRAIN
RESEARCH**

Research report

Reduced retinal activity increases GFAP immunoreactivity in rat lateral geniculate nucleus

Karen S. Canady^a, Jaime F. Olavarria^b, Edwin W Rubel^{a,b,*}

^a Virginia Merrill Bloedel Hearing Research Center, Department of Otolaryngology-HNS, RL-30, University of Washington, Seattle, WA 98195, USA

^b Department of Psychology, NI-25, University of Washington, Seattle, WA 98195, USA

Accepted 9 August 1994

Abstract

Dynamic regulation of astrocytic processes by the electrical activity of local neurons has been previously described in chick cochlear nucleus. The present study extends this observation by showing that astrocytes in the rat lateral geniculate nucleus (LGN) also increase their immunoreactivity for glial fibrillary acidic protein (GFAP) soon after deprivation of afferent visual neuronal activity. Within 6 h of enucleation, which eliminates a major source of afferent input to the contralateral LGN, GFAP immunoreactivity increases relative to the ipsilateral LGN. A similar increase in GFAP immunoreactivity can be induced by intraocular injections of tetrodotoxin, demonstrating that a reversible manipulation of optic nerve electrical activity is sufficient to regulate LGN astrocytes. This rapid response to activity deprivation is less dramatic than the gliotic reaction observed 3 weeks following deafferentation, by which time afferent terminals have degenerated. These results support the notion that regulation of astrocytic processes by neural activity may play an important role in activity-dependent synaptic regulations in the various sensory systems of vertebrates.

Keywords: Glia; Astrocyte; Plasticity; Visual system; Deprivation; Afferent activity

1. Introduction

The plasticity that astrocytes show in their morphology and function makes these glial cells likely players in the modulation of neural structure and function [10,16,25]. Astrocytes express voltage-sensitive ion channels [1] and have receptors for neurotransmitters such as glutamate [24]. Structural changes in astrocytes have been associated with synaptic regulation [4,14], and it has been suggested that astrocytic responses to afferent transmitter release are essential to the survival of developing spinal neurons *in vitro* [2]. Thus, it appears that the role of astrocytes in the regulation of neural function extends beyond the long-recognized response to injury [13,18].

Our recent work has shown that the increased expression of glial fibrillary acidic protein (GFAP) ob-

served following deafferentation may reflect, in part, a dynamic responsiveness of astrocytes to changes in neuronal electrical activity. Rubel and MacDonald [19] showed that increases in GFAP-immunopositive and silver-impregnated glial processes in chick nucleus magnocellularis occur within 4–6 h of cochlea removal, too rapidly to be initiated by degeneration of afferent terminals. Canady and Rubel [3] used intralabyrinthine tetrodotoxin (TTX) injections to block electrical activity in these afferents and found that activity blockade was sufficient to induce increased immunoreactivity for GFAP. Not only was blockade of afferent activity sufficient to increase GFAP immunoreactivity in nucleus magnocellularis, but the subsequent resumption of electrical activity resulted in a recovery to normal levels of GFAP immunoreactivity [3]. These prior results suggest that: (1) reduced electrical activity may contribute to glial reactions to neuropathological conditions, and (2) variations in neuronal activity under physiological conditions may modify the structure of local glial cells.

* Corresponding author at address a. Fax: (1) (206) 543-5152; e-mail: rubel@u.washington.edu

The results from the chick auditory system raise the question of whether regulation of astrocytic structure by neuronal activity occurs in other neuronal systems and other species. In the present study, we examined the astrocytic response to reduced neuronal activity in the lateral geniculate nucleus (LGN) of rats. The rat LGN was selected to take advantage of the highly crossed retinal projection in this species [20], which largely restricts the effects of experimental manipulations in one eye to the contralateral LGN, while keeping the ipsilateral LGN relatively unaffected. Thus, the effects of monocular manipulations can be evaluated within individual animals and within the same tissue sections.

Astrocytic immunoreactivity for GFAP was examined in the rat LGN at short intervals following either enucleation or suppression of optic nerve activity. First, the time course of glial changes in rat LGN following afferent manipulation was determined by examining GFAP immunoreactivity 3 h to 3 weeks following unilateral enucleation. Another group of rats was examined after unilateral intraocular TTX injection to determine if suppression of electrical activity in LGN is sufficient to increase GFAP immunoreactivity. We report that enucleation results in increased GFAP immunoreactivity in rat LGN within 6 h and that reduced afferent electrical activity is sufficient to elicit a similar increase in GFAP immunoreactivity. Some of these results have been presented previously in abstract form [5].

2. Materials and Methods

The present study is based on data from 34 female rats of the Long-Evans strain weighing 200–300 g. Twenty-three of these rats were subjected to monocular enucleation, 4 rats received intraocular injections of TTX, and 7 rats served as unoperated controls. In addition, we also examined two rats that survived one week after monocular injection of TTX. With the exception of three left-eye enucleates, all of the enucleates had the right eye removed. All of the TTX injections were done on the right side.

Prior to the surgical procedures, rats were anesthetized by either inhalation of halothane (2% in air) or intraperitoneal injection of Equithesin (9.8 mg/ml sodium pentobarbital, 42.5 mg/ml chloral hydrate, 21.3 mg/ml magnesium sulfate, in 12% ethanol, 44% propylene glycol). Rats were monitored postoperatively while resting under a heat lamp until fully recovered from anesthesia. Enucleated rats were sacrificed at the following postoperative intervals: 3 h ($n = 8$), 6 h ($n = 7$), 12 h ($n = 5$), and 3 weeks ($n = 3$). Rats treated with TTX were sacrificed after the second of two injections, given 3.5 h apart.

2.1. TTX injection

Using a 10 μ l Hamilton syringe, 2 μ l of 3 mM TTX were injected into one eye over a period of 10 min. The needle was left in place for an additional 10 min to minimize leakage from the injection site. The effectiveness of the injections was evaluated by eliciting the pupillary reflex to light in a dark room. Failure of the pupil to constrict

indicated a successful TTX injection [7,26]. This test was repeated at short intervals and, as soon as a partial constriction was detected, a second injection of 2 μ l of 3 mM TTX was given. In all cases, this occurred at 3.5 h after the first injection. All surgical procedures were performed according to protocols approved by the University of Washington Animal Care Committee.

2.2. Histology and immunocytochemistry

At the end of their assigned survival periods, rats were deeply anesthetized with 0.3 ml sodium pentobarbital (Nembutal, 50 mg/ml, i.p.) and perfused transcardially with 0.9% saline followed by 4% paraformaldehyde in 0.1 M phosphate buffer. Brains were removed, blocked, dehydrated in a graded series of ethanols, cleared overnight in methyl salicylate and embedded in paraffin. Coronal sections through the LGN were cut at 10 μ m and a 1 in 10 series was mounted onto poly-L-lysine-coated glass slides. After sections were deparaffinized and rehydrated, immunocytochemistry was performed using a Vectastain ABC kit (Vector Labs, Burlingame, CA) and standard methods [3]. Sections were incubated overnight at room temperature in a polyclonal antiserum to bovine GFAP (DAKO, Santa Barbara, CA) diluted 1:1200. Diaminobenzidine (Sigma, St. Louis, MO) was used as the chromogen.

A series of adjacent tissue sections was also mounted onto poly-L-lysine-coated glass slides and stained for myelin. The deparaffinized and rehydrated sections were first immersed in filtered 10% ferric ammonium sulfate for 30 min. After two washes in deionized water, the sections were immersed for 4–6 h in stain solution (10% filtered, 10% w/v alcoholic hematoxylin, and 7% w/v filtered, saturated lithium carbonate). These myelin-stained sections were used to identify LGN borders for data analysis.

2.3. Data analysis

The relative intensity of GFAP immunolabeling in LGN ipsilateral and contralateral to activity blockade was analyzed using a BioQuant Image Analysis system (R&M Biometrics, Nashville, TN) in a manner similar to that used by Canady and Rubel [3]. Four nonadjacent sections per animal were analyzed using a 40 \times objective on a Leitz Aristoplan microscope. The microscopic image was relayed by a Dage MTI CCD 72 video camera to a video monitor.

Sections selected for measurement appeared evenly stained, were symmetric in the transverse plane and contained sufficiently central portions of LGN so that three non-overlapping measurements could be taken on each side of the brain. The border of the LGN was determined by closely inspecting adjacent sections stained for myelin. For each side of each section, one measurement was taken along the ventrolateral border of LGN, one in the center, and one dorsomedial to the central measurement. Each measurement was made from a roughly rectangular area ($\sim 180 \mu\text{m} \times \sim 120 \mu\text{m}$). The three diagonally aligned rectangles covered well over half of the cross-sectional area of LGN.

The microdensitometry system was set up to scan the selected area of the digitized image and recognize pixels of the image whose optical density exceeded a pre-determined threshold. The threshold was selected to detect intensely stained astrocytic processes. The same threshold, as well as the same microscope and video camera settings, was used for both the experimental and control sides of each tissue section. Because immunocytochemical staining intensity can vary across identically-treated sections, the threshold setting must be adjusted for each section to achieve a consistent level of detection. Otherwise, the same absolute threshold could detect 20% of the area of a darkly-stained nucleus and only 0.5% of a lightly-stained nucleus. Thus, quantitative comparisons can only be made between sides of individual tissue sections (using the same threshold), and not between animals. For example, a difference in immunoreac-

tivity between the experimental LGN of one group and the experimental LGN of another group cannot be quantified.

For each sampling area, the fraction containing suprathreshold pixels was calculated and expressed as a percentage of the sampling area. The three values obtained for each side were then averaged. The percent difference in area density of suprathreshold pixels between the contralateral and ipsilateral LGNs was then averaged across the four tissue sections for each animal. A positive value for the mean percent difference indicates more GFAP+ astrocytic processes on the experimental (deafferented or deprived) side of the brain. The statistical significance of measured differences was assessed using one-way ANOVA.

3. Results

3.1. Control animals

Sections from unoperated control animals show sparse labeling within LGN as compared to adjacent neural regions. Labeling is found on both classically stellate astrocytes, and on what appear to be bits and pieces of astrocytic processes, perhaps caught in the section as they pass through at varied angles. The distribution of labeling appears somewhat uneven across the nucleus, and no consistent distribution pattern of label is found across sections. The medial portion of LGN, for example, cannot be distinguished on the basis of GFAP immunoreactivity. The pial surface is always well-labeled and several bands of label are often found parallel to the pial border. (This region

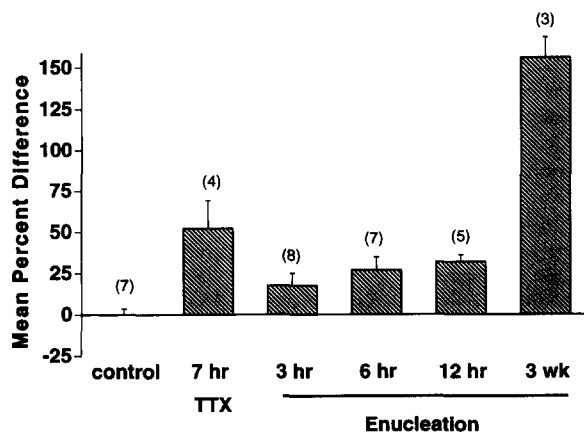


Fig. 1. Mean percent difference in area density of GFAP immunoreactivity between the activity-deprived LGN as compared to the control LGN on the contralateral side of the same tissue section. Positive values indicate more immunoreactivity on the experimental side of the brain. Error bars represent standard error of the mean. The mean for each group, except the 3 h group, is significantly greater ($P < 0.01$) than that of the control group. The mean for the 7 h group is significantly greater ($P < 0.05$) than the mean for the 3 h group, and the 3 week group mean is significantly greater ($P < 0.01$) than all other means. Control refers to unoperated, control animals.

was omitted from the data analysis.) No differences were observed between the LGN on the two sides of the brain. For the seven control animals, the mean percent difference in area density of suprathreshold pixels between the two sides of the brain was 0.1 (S.E.M. = 3.5%). The results of the data analysis are plotted in Fig. 1. Data from the two rats that survived one week after an intraocular TTX injection was not significantly different from the unoperated controls, indicating that the injection procedure per se did not cause significant retinal damage.

3.2. Enucleated animals

By 3 h following enucleation, small differences in GFAP immunoreactivity between the ipsilateral and contralateral LGNs can be measured. Increased GFAP immunoreactivity in the LGN contralateral to enucleation is barely detectable through casual microscopic observation in sections from most 3 h animals, and not detectable in some. The increase in GFAP immunoreactivity appears in patches distributed randomly throughout the LGN. Many GFAP+ processes in the experimental LGN appear thicker than most of the processes found in the control LGN on the contralateral side. The BioQuant analysis revealed a difference in mean suprathreshold GFAP immunoreactivity of 17.5% (S.E.M. = 7.6) on the experimental side as compared to the contralateral LGN, but this difference was not statistically significant ($P < 0.10$).

At 6 h after enucleation, increased GFAP immunoreactivity in the experimental LGN is apparent in sections from most animals. As observed in the 3 h animals, the GFAP immunoreactivity on the experimental side appears patchy, but covers more of the LGN because of the size and number of patches of GFAP+ processes. Again, no pattern to the distribution of immunolabel is apparent. The difference in area density of GFAP immunoreactivity averages 27% greater (S.E.M. = 7.9) in the experimental LGN as compared to the opposite LGN, and is statistically significant ($P = 0.01$).

By 12 h following enucleation, increased GFAP immunoreactivity in the experimental LGN is readily apparent and consistent across sections and across animals (Fig. 2). The labeling pattern is similar to that found in shorter-term enucleates, but there are more and thicker GFAP+ processes. The mean increase in area density of GFAP immunoreactivity is 32% (S.E.M. = 4.2). This difference is statistically significant ($P < 0.01$).

Three weeks after enucleation, the LGN on both sides of the brain has numerous thick and heavily branched GFAP+ processes, with far more and thicker processes appearing in the experimental LGN (Fig. 3). The mean increase in area density of GFAP im-

munoreactivity for the 3 animals studied 3 weeks after enucleation is 156% (S.E.M. = 12.4) and is statistically significant ($P < 0.001$). Although quantitative compar-

isons of immunocytochemical labeling between animals cannot be made, a consistent qualitative difference between the control LGNs of enucleates and the LGNs

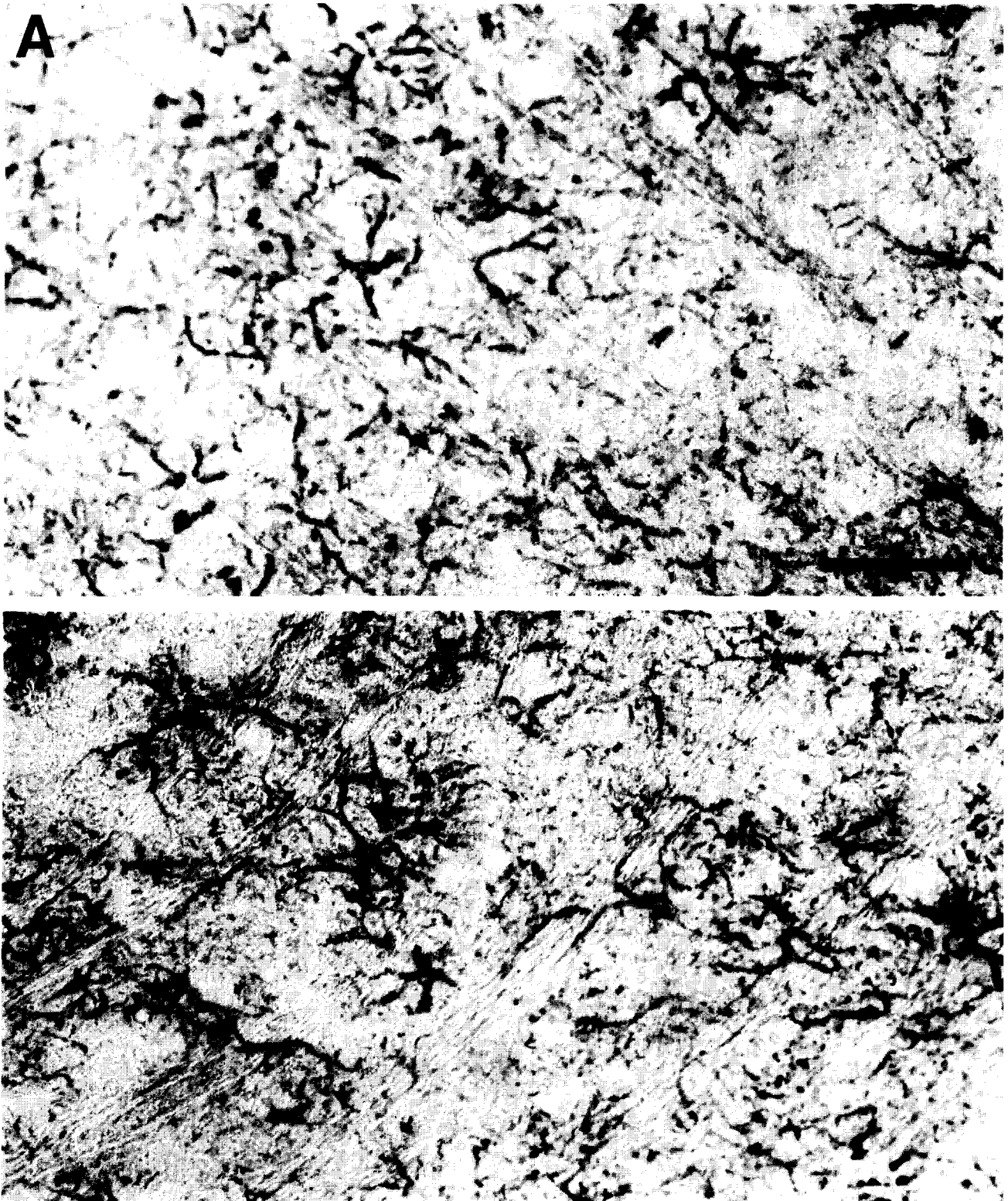


Fig. 2. Dorsal LGN at 12 h after monocular enucleation, immunostained for GFAP. A: control side, ipsilateral to enucleation. B: experimental, contralateral side of same tissue section. Note increased amount of GFAP-immunopositive processes. Bar = 50 μ m.

of unoperated animals is observed. An increased number of thick and heavily branched GFAP positive processes is clearly apparent in the control LGNs of 3

week enucleates, and consistently appears to a less dramatic extent in the control LGNs of short-term enucleates.



Fig. 3. Dorsal LGN at 3 weeks after monocular enucleation, immunostained for GFAP. A: control side, ipsilateral to enucleation. B: experimental, deafferented LGN, from contralateral side of same tissue section. Note increased amount of GFAP immunopositive processes on both sides of the brain, with dramatically increased quantity and thickness of processes on deafferented side. Bar = 50 μ m.

3.3. TTX animals

Tissue from the animals studied after 7 h of TTX treatment show clear differences in GFAP staining

between experimental and control sides. The mean difference in area density of GFAP immunoreactivity is 52.3% (S.E.M. = 16.9) and is statistically significant ($P < 0.001$). Interestingly, the absolute values of GFAP

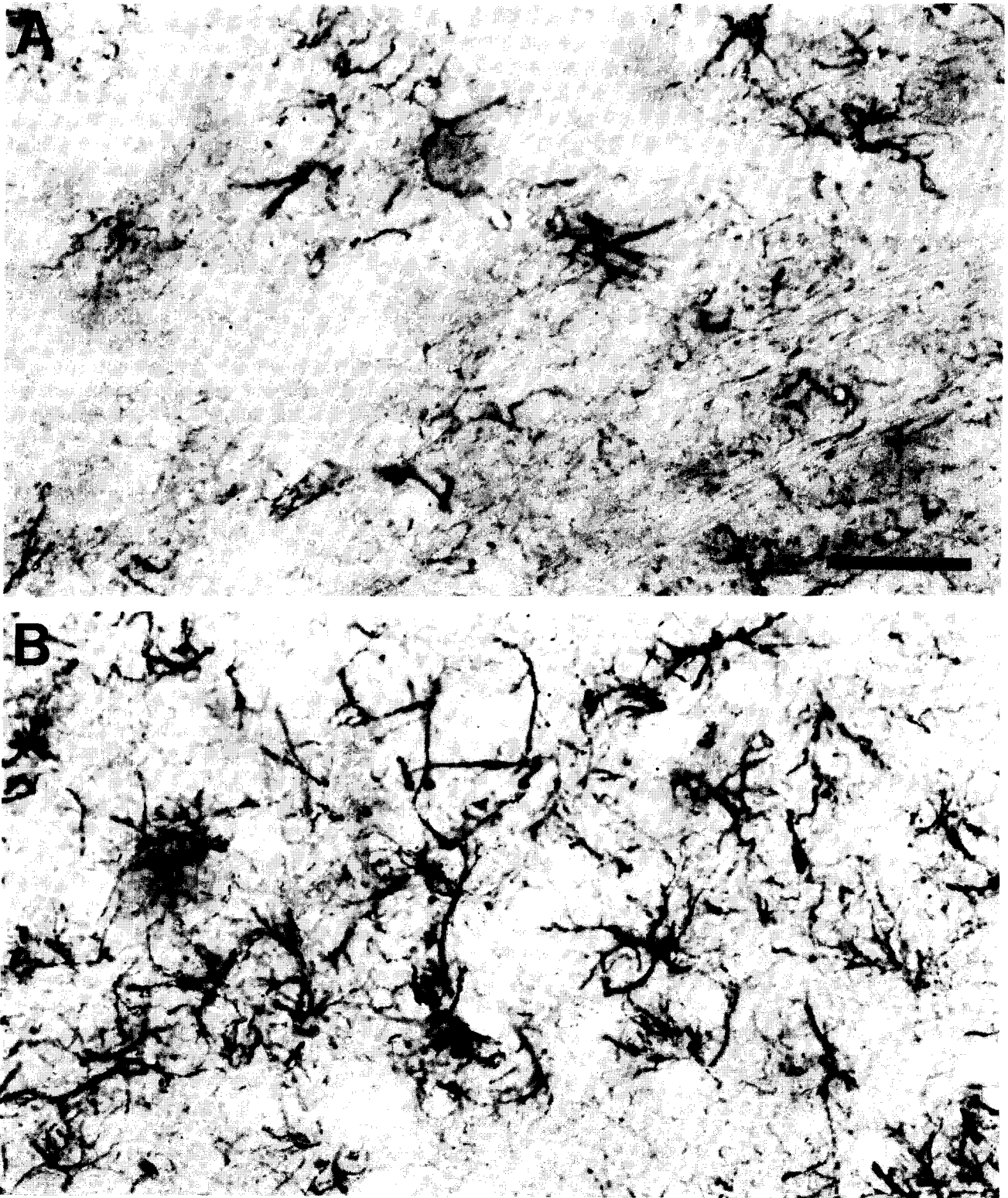


Fig. 4. Dorsal LGN after 7 h of monocular activity blockade, immunostained for GFAP. A: control side, ipsilateral to TTX treatment. B: experimental LGN, from contralateral side of same tissue section. Note increased amount of GFAP-immunopositive processes on activity-deprived side and sparse labeling on the control side. Bar = 50 μ m.

immunoreactivity in both the contralateral and ipsilateral LGNs appear to be less in TTX-treated animals than in enucleates (Fig. 4). The ipsilateral, control LGN of TTX-treated rats appears more like the LGN of control animals (data not shown) in that the sparse GFAP immunoreactivity is distributed in patches throughout the nucleus. Whether this difference in constitutive staining levels reflects random variation in the immunocytochemical staining or a bilateral effect of enucleation could not be determined.

4. Discussion

The present results show that astrocytic GFAP immunoreactivity in the rat visual thalamus, as in the chick cochlear nucleus, can be rapidly regulated by altered afferent neuronal activity. These results suggest that rapid regulation of glial cell structure by afferent neuronal input may be a general phenomenon across different species and neural systems. Additional evidence in support of this idea comes from studies showing that glial upregulation of GFAP in response to short-term neuronal activity blockade also occurs in perisynaptic Schwann cells at the frog neuromuscular junction [9].

While nerve stimulation prevents the GFAP upregulation in both the chick nucleus magnocellularis (NM) and at the frog neuromuscular junction, these activity-dependent glial responses appear to operate by different mechanisms. In the chick, the GFAP increase is prevented by any form of neuronal depolarization: orthodromic, antidromic, or orthodromic with transmitter release blocked by a low-calcium medium [4]. In contrast, GFAP upregulation at the frog neuromuscular junction cannot be prevented by nerve stimulation when neurotransmitter release is blocked. Thus, although GFAP upregulation in response to neuronal activity blockade appears to be common to a variety of species and neural systems, this regulation may occur through a variety of mechanisms.

The increased GFAP immunoreactivity observed in the present study reveals a change in astrocytic processes of the LGN receiving reduced afferent activation. The methods used in the present study do not provide measures of absolute levels of GFAP immunoreactivity, which would indicate, for example, whether there is a contralateral effect of enucleation. Likewise, the methods employed here do not measure the extent of variation above and below the detection threshold. The only quantitative comparisons we can make are of relative changes in GFAP immunoreactivity between the treated and untreated sides of individual tissue sections.

The increased GFAP immunoreactivity observed in the present study could result from increased synthesis

of GFAP and distribution within existing processes, through a proliferation of processes, by assembly or disassembly of intermediate filaments, by altered protein phosphorylation, by glial process swelling, or through a combination of these events. Based on our previous studies of the rapid glial reaction to activity blockade in the chick NM, it is likely that the increased GFAP immunoreactivity observed in the rat LGN reflects a proliferation of astrocytic processes. The three-dimensional reconstruction of silver-impregnated glial cells by Rubel and MacDonald [19] revealed a 91% increase in glial process length and a 110% increase in the number of glial processes per cell in the NM of chicks sacrificed 4–6 h after cochlea removal. In that study, chicks studied 6 h after cochlea removal also showed an 84% increase in GFAP immunoreactivity. More recently, we have studied electron micrographs taken from the NM of chicks sacrificed 6 h after cochlea removal [4]. We find a dramatic increase in the proportion of NM neuronal surface apposed by glial versus neuronal membrane. Considered together, these studies suggest that the increased GFAP immunoreactivity observed in the rat LGN after brief disruptions of afferent input represents a proliferation and repositioning of astrocytic processes along with a redistribution or synthesis of GFAP protein.

The dramatic qualitative and quantitative differences between the short-term enucleated animals and the 3-week enucleates may reflect the difference between a reversible glial response to changes in neuronal activity and a permanent gliotic reaction to neuronal degeneration. Similar differences were observed in the chick NM at 3 h versus 3 days after cochlea removal. In the chick NM, afferent terminal degeneration, postsynaptic neuronal atrophy and transneuronal death are complete by 3 days after cochlea removal. The increase in GFAP immunoreactivity is also far greater at 3 days than at 3 h after cochlea removal, due to increases in both the number of intensely stained processes and glial cell proliferation [12,19]. The increase in GFAP immunoreactivity observed after 3 h of afferent activity blockade, however, can be reversed by the resumption of neuronal activity [3].

The greater percent difference in area density of GFAP immunoreactivity between the activity-deprived and control sides of the brain for TTX-treated animals as compared to enucleates (Fig. 1) may reflect the differences observed between the control LGNs of these two groups. The control side of the brain for TTX-treated rats had the sparse pattern of GFAP immunoreactivity found in the LGNs of unoperated animals. This differed from the control side of enucleates in which we noted a qualitative pattern of slightly more patches of thicker and more immunoreactive glial processes. This trend toward elevated GFAP immunoreactivity in the control LGN of enucleates was

far more dramatic in the 3-week enucleates as compared to the short-term enucleates (Figs. 2 and 3). Glial reactions contralateral to a deafferented region have been reported at one or more days post-lesion in the hippocampus [8,22] and visual cortex [11]. Thus, any bilateral effects of deafferentation may begin in moderate form during the first hours. If there are early ipsilateral effects of deafferentation on astrocytes in the rat LGN, however, they are apparently not induced by activity blockade alone.

The sensitivity of astrocytic morphology to altered neuronal activity may be an important component of activity-dependent neural modifications. The potential for glial involvement in synaptic reorganization has been suggested by in vitro studies of cerebellar explants [14] and by in vivo studies of parasympathetic ganglia [17]. The in vitro studies show an increase in synaptic contacts when the glial population is reduced, while the in vivo studies show that glial cells do not remain stationary over time.

In the visual system, there are numerous examples of rapid and reversible changes in neuronal properties induced by various forms of sensory deprivation during development (e.g., see Refs. 15, 21, 23). For example, Chino et al. [6] have recently reported substantial reorganization of the retinotopic map in adult cat visual cortex within hours of monocular enucleation. It is possible that these functional changes are mediated, at least in part, by dynamic changes in astrocytic processes induced by altered neuronal activity. For instance, labile astrocytic processes could help modulate the effectiveness of synapses by inserting themselves between inactive terminals and their targets, as well as by releasing newly active terminals from electrical isolation.

Acknowledgements

This work was supported by PHS Grants 00520 (to E.W.R.) and EY09343 (to J.F.O.). We thank Paul Schwartz and Janet Clardy for expert photographic assistance.

References

- [1] Barres, B.A., Chun, L.L.Y. and Corey, D.P., Ion channels in vertebrate glia, *Annu. Rev. Neurosci.*, 13 (1990) 441–474.
- [2] Brenneman, D.E., Neale, E.A., Foster, G.A., d'Autremont, S.W. and Westbrook, G.L., Nonneuronal cells mediate neurotrophic action of vasoactive intestinal peptide, *J. Cell Biol.*, 104 (1987) 1603–1610.
- [3] Canady, K.S. and Rubel, E.W., Rapid and reversible astrocytic reaction to afferent activity blockade in chick cochlear nucleus, *J. Neurosci.*, 12 (1992) 1001–1009.
- [4] Canady, K.S., Hyson, R.L. and Rubel, E.W., The astrocytic response to afferent activity blockade in chick nucleus magnocellularis is independent of synaptic activation, age and neuronal survival, *J. Neurosci.*, (1994) in press.
- [5] Canady, K.S., Olavarria, J.F. and Rubel, E.W., Rapid increase in astrocytic GFAP immunoreactivity in LGN of enucleated rats, *Soc. Neurosci. Abstr.*, 18 (1992) 1310.
- [6] Chino, Y.M., Kaas, J.H., Smith, E.L. III, Langston, A.L. and Cheng, H., Rapid reorganization of cortical maps in adult cats following restricted deafferentation in retina, *Vision Res.*, 32 (1992) 789–796.
- [7] Dubin, M.W., Stark, L.A. and Archer, S.M., A role for action potential activity in the development of neuronal connections in the kitten retino-geniculate pathway, *J. Neurosci.*, 6 (1986) 1021–1036.
- [8] Gall, C., Rose, G. and Lynch, G., Proliferative and migratory activity of glial cells in the partially deafferented hippocampus, *J. Comp. Neurol.*, 183 (1979) 539–550.
- [9] Georgiou, J., Robitaille, R., Trimble, W.S. and Charlton, M.P., Synaptic regulation of glial protein expression in vivo, *Neuron*, 12 (1994) 443–455.
- [10] Giulian, D., Vaca, K. and Corpuz, M., Brain glia release factors with opposing actions upon neuronal survival, *J. Neurosci.*, 13 (1993) 29–37.
- [11] Hajós, F., Kálmán, M., Zilles, K., Schleicher, A. and Sotonyi, P., Remote astrocytic response as demonstrated by glial fibrillary acidic protein immunohistochemistry in the visual cortex of dorsal lateral geniculate nucleus lesioned rats, *Glia*, 3 (1990) 301–310.
- [12] Lurie, D.I. and Rubel, E.W., Astrocyte proliferation in the chick auditory brainstem following cochlea removal, *J. Comp. Neurol.*, (1994) in press.
- [13] Malhotra, S.K., Shnitka, J.K. and Elbrink, J., Reactive astrocytes—a review, *Cytobios*, 61 (1990) 133–160.
- [14] Meshul, K.D., Frederick, J.S. and Herndon, R.M., Astrocytes play a role in regulation of synaptic density, *Brain Res.*, 402 (1987) 139–145.
- [15] Movshon, J.A. and Van Sluyters, R.C., Visual Neural Development, *Annu. Rev. Psychol.*, 32 (1981) 477–522.
- [16] Müller, C.M., A role for glial cells in activity-dependent central nervous plasticity? Review and hypothesis, *Int. Rev. Neurobiol.*, 34 (1992) 215–281.
- [17] Pomeroy, S.L. and Purves, D., Neuron/glia relationships observed over intervals of several months in living mice, *J. Cell Biol.*, 107 (1988) 1167–1175.
- [18] Reier, P.J., Gliosis following CNS injury: the anatomy of astrocytic scars and their influences on axonal elongation. In S. Federoff and A. Vernadakis (Eds.), *Astrocytes, Vol. 3*, Academic Press, Orlando, 1986, pp. 263–324.
- [19] Rubel, E.W. and MacDonald, G.H., Rapid growth of astrocytic processes in n. magnocellularis following cochlea removal, *J. Comp. Neurol.*, 318 (1992) 415–425.
- [20] Sefton, A.J. and Dreher, B., Visual system. In G. Paxinos (Ed.), *The Rat Nervous System, Vol. 1, Forebrain and Midbrain*, Academic Press, Orlando, 1985, pp. 169–221.
- [21] Sherman, S.M., and Spear, P.D., Organization of visual pathways in normal and visually deprived cats, *Physiol. Rev.*, 62 (1982) 738–855.
- [22] Steward, O., Torre, E.R., Phillips, L.L. and Trimmer, P.A., The process of reinnervation in the dentate gyrus of adult rats: time course of increases in mRNA for glial fibrillary acidic protein, *J. Neurosci.*, 10 (1990) 2373–2384.

- [23] Stryker, M.P. and Harris, W.A., Binocular impulse blockade prevents the formation of ocular dominance columns in cat visual cortex, *J. Neurosci.*, 6 (1986) 2117–2133.
- [24] Teichberg, V.I., Glial glutamate receptors: likely actors in brain signaling, *FASEB J.*, 5 (1991) 3086–3091.
- [25] Theodosios, D.T. and Poulain, D.A., Neuronal-glial and synaptic remodeling in the adult hypothalamus in response to physiological stimuli, *Ciba Found. Symp.*, 168 (1992) 209–225.
- [26] Thurlow, G.A. and Cooper, R.M., Activity-dependent changes in eye influence during monocular blockade: increases in the effects of visual stimulation on 2-DG uptake in the adult rat geniculostriate system, *J. Comp. Neurol.*, 306 (1991) 697–707.